Datasheet for 600-103-215

GFP Antibody Peroxidase Conjugate

Overview

Description:	Anti-GFP (GOAT) Antibody Peroxidase Conjugated Min X Hu Ms and Rt Serum Proteins - 600-103-215
Item No.:	600-103-215
Size:	1 mg
Applications:	ELISA, WB, IF, IHC, IP, Multiplex
Reactivity:	GFP, eGFP, rGFP
Host Species:	Goat

Product Details

Background:	HRP Anti-GFP is ideal for western blotting, ELISA and Immunohistochemistry. Green fluorescent protein is a 27 kDa protein produced from the jellyfish Aequorea victoria, which emits green light (emission peak at a wavelength of 509nm) when excited by blue light. GFP is an important tool in cell biology research. GFP is widely used enabling researchers to visualize and localize GFP-tagged proteins within living cells without the need for chemical staining.
Synonyms:	goat anti-GFP Antibody peroxidase Conjugation, HRP conjugated goat anti-GFP antibody, Green Fluorescent Protein, GFP antibody, Green Fluorescent Protein antibody, EGFP, enhanced Green Fluorescent Protein, Aequorea victoria, Jellyfish
Host Species:	Goat
Conjugate:	Peroxidase (HRP)
Clonality:	Polyclonal
Format:	IgG

Target Details

Reactivity:	GFP, eGFP, rGFP
Immunogen Type:	Recombinant Protein
Immunogen:	Recombinant Green Fluorescent Protein (GFP) fusion protein corresponding to the full length amino acid sequence (246aa) derived from the jellyfish Aequorea victoria.

Purity/Specificity:	Anti-GFP antibody was prepared from monospecific antiserum by immunoaffinity chromatography using Green Fluorescent Protein (Aequorea victoria) coupled to agarose beads followed by solid phase adsorption(s) to remove any unwanted reactivities. Assay by immunoelectrophoresis resulted in a single precipitin arc against anti-Goat Serum, anti-Peroxidase and purified and partially purified Green Fluorescent Protein (Aequorea victoria). No reaction was observed against Human, Mouse and Rat Serum Proteins.
Relevant Links:	• 600-103-215 SDS • UniProtKB - P42212

Application Details

Tested Applications:	ELISA, WB
Suggested Applications:	IF, IHC, IP, Multiplex (Based on references)
Application Note:	Polyclonal anti-GFP is designed to detect GFP and its variants. Anti-GFP Peroxidase conjugated antibody has been tested by ELISA to detect GFP by ELISA (sandwich or capture) for the direct binding of antigen and recognizes wild type, recombinant and enhanced forms of GFP and by western blot. Biotin conjugated polyclonal anti-GFP used in a sandwich ELISA is well suited to titrate GFP in solution using this antibody in combination with Rockland's monoclonal anti-GFP (600-301-215) using either form of the antibody as the capture or detection antibody. However, use the monoclonal form only for the detection of wild type or recombinant GFP as this form does not sufficiently detect 'enhanced' GFP. The detection antibody is typically conjugated to biotin and subsequently reacted with streptavidin conjugated HRP (code # S000-03). Fluorochrome conjugated polyclonal anti-GFP can be used to detect GFP by immunofluorescence microscopy in prokaryotic (E.coli) and eukaryotic (CHO cells) expression systems and can detect GFP containing inserts. Significant amplification of signal is achieved using fluorochrome conjugated polyclonal anti-GFP relative to the fluorescence of GFP alone. For immunoblotting use either alkaline phosphatase or peroxidase conjugated polyclonal anti-GFP to detect GFP or GFP containing proteins on western blots. Optimal titers for applications should be determined by the researcher.
Assay Dilutions:	All assays should be optimized by the user. Recommended dilutions (if any) may be listed below.
ELISA:	1:10,000 - 1:50,000
IHC:	1:500 - 1:2,000
WB:	1:2,000 - 1:5,000

Formulation

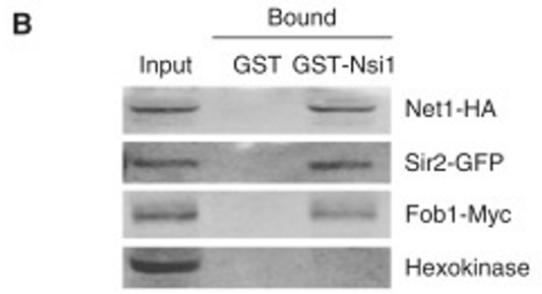
Physical State:	Lyophilized
Concentration:	1.0 mg/mL by UV absorbance at 280 nm

Buffer:	0.02 M Potassium Phosphate, 0.15 M Sodium Chloride, pH 7.2
Preservative:	0.01% (w/v) Gentamicin Sulfate. Do NOT add Sodium Azide!
Stabilizer:	10 mg/mL Bovine Serum Albumin (BSA) - Immunoglobulin and Protease free
Reconstitution Volume:	1.0 mL
Reconstitution Buffer:	Restore with deionized water (or equivalent)

Shipping & Handling

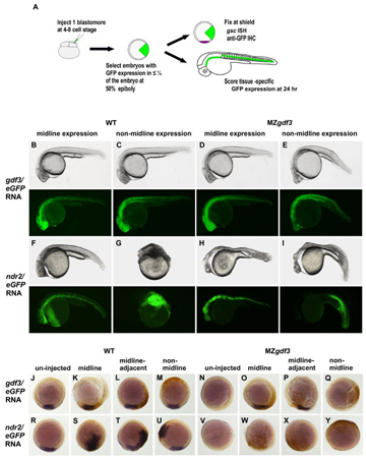
Shipping Condition:	Ambient
Storage Condition:	Store GFP antibody at 4° C prior to restoration. For extended storage aliquot contents and freeze at -20° C or below. Avoid cycles of freezing and thawing. Centrifuge product if not completely clear after standing at room temperature. This product is stable for several weeks at 4° C as an undiluted liquid. Dilute only prior to immediate use.
Expiration:	Expiration date is one (1) year from date of receipt.

Images

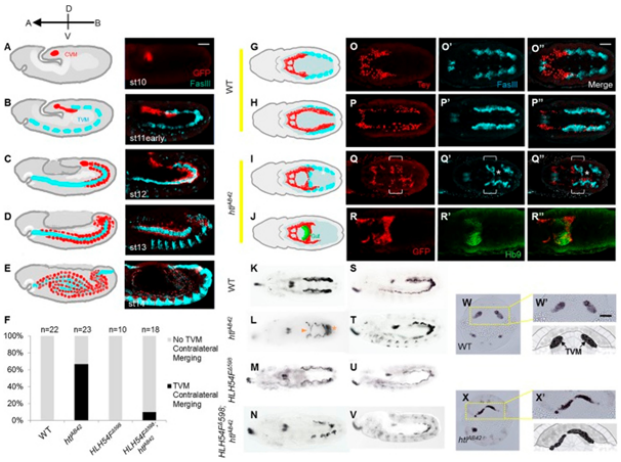


Western Blot
(B) GST pull-down assay showing direct association of Nsi1 with Net1, Sir2 and Fob1. GST-Nsi1 associates with Net1, Sir2 and Fob1 from whole cell extracts (left panel). GST-Sir2 and GST-Fob1 associate with Nsi1 from whole cell extracts (right panel). Fig 3. PMID: 22362748

Immunohistochemistry
The site of ectopic Nodal/Gdf3 signaling influences the efficacy of MZgdf3 mutant rescue and the severity of overexpression phenotypes in WT embryos. (A) Experimental Approach: 4–8 cell WT and MZgdf3 embryos were injected with 5 pg ndr2 RNA +25 pg eGFP RNA or with 50 pg gdf3 RNA +25 pg eGFP RNA. At 50% epiboly embryos expressing eGFP in 25% or less of the blastoderm were selected. These embryos were grown until 24 hpf and

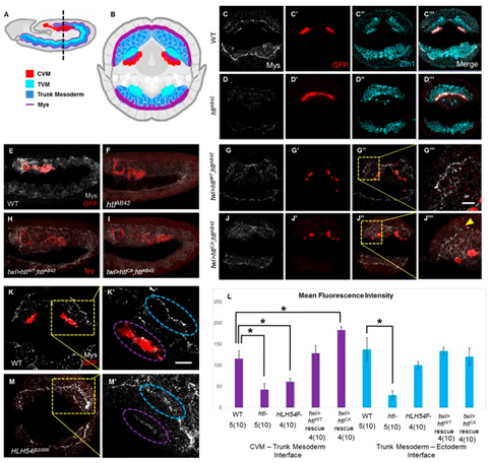


photographed with transmitted light and fluorescent illumination or were grown until shield stage and processed by WISH with a gsc probe then by IHC with anti-GFP. (B, C) 24 hpf WT embryos injected with gdf3/eGFP RNA had normal phenotypes, regardless of whether (B) midline or (C) non-midline lineages were targeted. (D) MZgdf3 embryos expressing Gdf3/eGFP in dorsally-derived midline lineages including the notochord and polster showed complete morphological rescue of notochord, somites, brain and eyes. (E) MZgdf3 embryos with expression of Gdf3/eGFP in non-midline lineages including the skin and somites showed rescue of somites and notochord but lacked normal development of anterior neural tissues and eyes. (F) Expression of Ndr2/eGFP in dorsal midline lineages in WT embryos resulted in embryos that were predominantly normal but some exhibited slightly narrower head and trunk and kinked notochords. This is strikingly distinct from (G) expression of Ndr2/eGFP outside midline lineages, which strongly dorsalized the embryos, or from ubiquitous expression in WT embryos injected with ndr2 RNA at the 1–2 cell stage (Figure 3S–U). (H, I) MZgdf3 embryos injected with ndr2/eGFP RNA showed no rescue of the MZgdf3 mutant phenotype regardless of what lineages were targeted. (J–Y) Shield stage embryos that were injected at the 4–8 cell stage with the indicated RNAs were processed by WISH for gsc and by IHC for GFP. Purple cells express gsc RNA; brown cells express GFP from RNA injection. Panels show embryos representative of each phenotypic class. (J–M) WT embryos at shield stage that were injected with gdf3/eGFP RNA showed no alteration in, or ectopic expression of gsc regardless of the location of expressing cells. (N–Q) MZgdf3 embryos injected with gdf3/eGFP RNA showed rescue of gsc expression when the expressing cells were located at (O), or adjacent to the presumptive dorsal shield (P). (R–U) WT embryos injected with ndr2/eGFP RNA showed ectopic gsc expression associated with the clone of expressing cells, regardless of the location of these cells within the embryo. (V–Y) MZgdf3 embryos injected with ndr2/eGFP RNA were unresponsive to this nodal ligand and showed no gsc expression. Note: Due to the lack of gsc expression, the location of the GFP-expressing clone of cells relative to the dorsal axis could not be reliably assigned in these embryos. Fig 4. PMID: 29140249



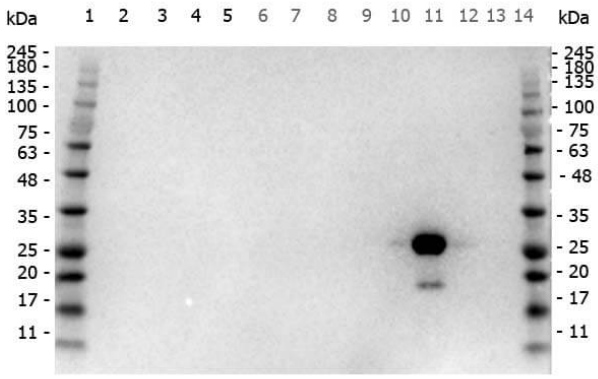
Immunofluorescence Microscopy

Loss of FGF results in severe CVM and TVM migration defects. (A-E) Immunofluorescence images and schematics illustrating CVM migration along the TVM over the course of development in sagittal views of wild-type (WT) embryos. CVM stained using anti-GFP (red) to label HLH54F-Gap-Venus reporter (HGV) or anti-FasIII (cyan) to stain TVM. (F) Graph summarizing incidence of contralateral merging defects in TVM, with gray bars indicating no merging defect and black bars indicating incidence of merging defect. (G,H,O-Q") Dorsal view of Stage 11 embryos of wild type (O-P") or htl mutants (Q-Q") and corresponding schematics (G,H,I) demonstrating bilateral migration of CVM cells along the TVM using antibodies against Tey (CVM, red) and FasIII (TVM, cyan); in htl mutants, midline crossing is observed in both the CVM and TVM (bracketed area), with ipsilateral gaps observed along the TVM (white asterisks; I,Q-Q"). (J,R-R") Dorsal view of Stage 11 htl mutant embryo demonstrating CVM midline crossing along the gut using antibodies against GFP (CVM, red) and Hb9 (gut, green). (K-N,S-V) Dorsal (K-N) and lateral (S-V) views of stage 11 wild-type (K,S), htlAB42 (L,T), HLH54FΔ598 (M,U) and HLH54FΔ598;htlAB42 (N,V) embryos immunostained using an anti-FasIII antibody. Orange arrowhead in L indicates contralateral merging of TVM tracks proximal to the gut, orange asterisk indicates posteriormost end, at which the contralateral TVM tracks are oriented most closely to each other. (W-X') Transverse cross-section and schematics of immunostained embryo illustrating the relative positions of TVM (FasIII, black) in wild type (W-W'), and contralateral merging in an htlAB42 mutant (X-X'). W' and X' show magnified views of W and X, respectively; schematic of W' and X' shown below, with TVM tissue shown in black. Scale bars: 40 µm in A-E,O-R"; 20 µm in W-X'. Fig 1.
PMID: 31239242



Immunofluorescence Microscopy

βPS1 myospheroid levels in the TVM are supported by FGF signaling and act to protect the TVM from CVM-driven contralateral merging. (A,B) Schematics illustrating relative positions of indicated tissues versus βPS1 (Mys) protein in sagittal (A) and transverse view (B). Dashed line in A indicates level of section in B. (C-D‴,G-G‴,J-J‴) Transverse cross-section of stage 11 embryos containing HGV GFP reporter (Stepanik et al., 2016) stained with anti-Mys, anti-GFP and anti-Zfh1 to identify βPS1, CVM and trunk mesoderm, respectively, in wild type (WT) (C-C‴ n=6; E, n=5), htl mutant (D-D‴, n=5; F, n=7) or upon expression of htlWT (G-G‴, n=5; H, n=5) or htlCA (I, n=5; J-J‴, n=4) via twi-GAL4 in htl mutants. Yellow arrowhead in J‴ indicates loss of polarized βPS1 expression at the trunk mesoderm-ectoderm interface. (E,F,H,I) Lateral posterior view of stage 11 embryos stained with anti-βPS1 and either anti-GFP (E,F) or anti-Tey (H,I) to identify CVM. (K-M') Transverse cross-sections and quantification of βPS1 protein expression levels as a function of mean fluorescence intensity values of 10 z-sections per sample (n, indicated below genotype label) with two ROIs quantified per sample: the CVM-TVM interface (purple dashed line and purple bars), and the trunk mesoderm-ectoderm interface (cyan dashed line and cyan bars). In HLH54F mutants that lack CVM, reduced βPS1 signal persists at what should have been the CVM-trunk mesoderm interface (L,M-M'). K' and M' show a higher magnification image of the boxed areas in K and M, respectively. Data are mean±s.d. *P<0.05 by one-way ANOVA. Scale bars: 20 µm. Fig 3. PMID: 31239242



Western Blot

Western Blot of Goat anti-GFP antibody Peroxidase conjugated. Marker: Opal Pre-stained ladder (p/n MB-210-0500). Lane 2: HEK293 lysate (p/n W09-000-365). Lane 3: HeLa Lysate (p/n W09-000-363). Lane 4: CHO/K1 Lysate (p/n W07-000-357). Lane 5: C2C12 Lysate. Lane 6: NIH/3T3 Lysate (p/n W10-000-358). Lane 7: Mouse Embryonic Fibroblast Lysate (p/n W10-001-371). Lane 8: E-coli HCP Control (p/n 000-001-J08). Lane 9: 2 Epitope MBP Tag Marker Lysate (p/n MB-301-0100). Lane 10: Recombinant Red Fluorescent Protein (p/n 000-001-379). Lane 11: Green Fluorescent Protein (p/n 000-001-215). Lane 12: Glutathione-S-Transferase Protein. Lane 13: Maltose Binding Protein (p/n 000-001-385). Marker: Opal Pre-stained ladder Load: 10 µg of lysate or 50ng of purified protein per lane. Primary antibody: goat anti-GFP peroxidase conjugated antibody at 1:1,000 overnight at 4C. Secondary antibody: none Blocking Buffer: BlockOut (p/n MB-073) for 30 min at RT. Predicted/Observed size: 28 kDa for GFP.

References

- Zamalutdinova SV et al. Using of transporter proteins to improve the uptake efficiency of hydrophobic compounds by Escherichia coli: a coordinated synthesis of START protein and P450scc system proteins to enhance cholesterol biotransformation. *Bioresour Bioprocess.* (2025)
- Lines M et al. The Dishevelled C-terminus interacts with the centrosomal protein Kizuna to regulate microtubule organization during ciliogenesis. *bioRxiv [Preprint].* (2025)
- Glomb O et al. A kinesin-1 adaptor complex controls bimodal slow axonal transport of spectrin in Caenorhabditis elegans. *Dev Cell.* (2023)
- Lee Y et al. Atg1-dependent phosphorylation of Vps34 is required for dynamic regulation of the phagophore assembly site and autophagy in Saccharomyces cerevisiae. *Autophagy.* (2023)
- Zhang Y et al. Sex-specific characteristics of cells expressing the cannabinoid 1 receptor in the dorsal horn of the lumbar spinal cord. *J Comp Neurol.* (2022)
- Devireddy S et al. Efficient progranulin exit from the ER requires its interaction with prosaposin, a Surf4 cargo. *J Cell Biol.* (2022)
- Maslakova AA et al. Towards unveiling the nature of short SERPINA1 transcripts: Avoiding the main ORF control to translate alpha1-antitrypsin C-terminal peptides. *Int J Biol Macromol.* (2022)
- Angarola B et al. LyTS: A Lysosome Localized Complex of TMEM192 and STK11IP. *bioRxiv Preprint* (2021)
- Devireddy S et al. Surf4 Promotes Endoplasmic Reticulum Exit of the Lysosomal Prosaposin-Progranulin Complex. *bioRxiv Preprint* (2021)

- Morshed S et al. TORC1 regulates ESCRT-0 complex formation on the vacuolar membrane and microautophagy induction in yeast. *Biochem Biophys Res Commun.* (2020)
- Del Rosario JS et al. Gi-coupled receptor activation potentiates Piezo2 currents via Gβγ. *EMBO Rep.* (2020)
- Stepanik V et al. FGF Pyramus Has a Transmembrane Domain and Cell-Autonomous Function in Polarity. *Curr Biol.* (2020)
- Lim G et al. Phosphoregulation of Rad51/Rad52 by CDK1 functions as a molecular switch for cell cycle–specific activation of homologous recombination. *Sci Adv.* (2020)
- Kim Y et al. Global analysis of protein homomerization in Saccharomyces cerevisiae. *Genome Res.* (2019)
- Macabenta F et al. Migrating cells control morphogenesis of substratum serving as track to promote directional movement of the collective. *Development.* (2019)
- Hennigan RF et al. Proximity biotinylation identifies a set of conformation-specific interactions between Merlin and cell junction proteins. *Sci Signal.* (2019)
- Atabekova AK et al. Mechanical stress-induced subcellular re-localization of N-terminally truncated tobacco Nt-4/1 protein. *Biochimie.* (2018)
- Sun J et al. FGF controls epithelial-mesenchymal transitions during gastrulation by regulating cell division and apicobasal polarity. *Development.* (2018)
- Bisgrove et al. Maternal Gdf3 is an obligatory cofactor in Nodal signaling for embryonic axis formation in zebrafish. *Elife* (2017)
- Gustin et al. Ebola Virus Glycoprotein Promotes Enhanced Viral Egress by Preventing Ebola VP40 From Associating With the Host Restriction Factor BST2/Tetherin. *The Journal of Infectious Diseases* (2015)
- Fahrenkamp et al. Src family kinases interfere with dimerization of STAT5A through a phosphotyrosine-SH2 domain interaction. *Cell Communication and Signaling* (2015)
- Botto et al. Kaposi Sarcoma Herpesvirus Induces HO-1 during De Novo Infection of Endothelial Cells via Viral miRNA-Dependent and -Independent Mechanisms. *mBio* (2015)
- Bejarano E et al. Connexins modulate autophagosome biogenesis. *Nat Cell Biol.* (2014)
- Chatain N et al. Src family kinases mediate cytoplasmic retention of activated STAT5 in BCR–ABL-positive cells. *Oncogene.* (2013)
- Sung MK et al. Genome-wide bimolecular fluorescence complementation analysis of SUMO interactome in yeast. *Genome Res.* (2013)
- Ha CW et al. Nsi1 plays a significant role in the silencing of ribosomal DNA in Saccharomyces cerevisiae. *Nucleic Acids Res.* (2012)
- Guarino E et al. Cdt1 proteolysis is promoted by dual PIP degrons and is modulated by PCNA ubiquitylation. *Nucleic Acids Res.* (2011)
- Sugita M et al. Molecular dissection of the butyrate action revealed the involvement of mitogen-activated protein kinase in cystic fibrosis transmembrane conductance regulator biogenesis. *Mol Pharmacol.* (2004)

Disclaimer

This product is for research use only and is not intended for therapeutic or diagnostic applications. Please contact a technical service representative for more information. All products of animal origin manufactured by Rockland Immunochemicals are derived from starting materials of North American origin. Collection was performed in United States Department of Agriculture (USDA) inspected facilities and all materials have been inspected and certified to be free of disease and suitable for exportation. All properties listed are typical characteristics and are not specifications. All suggestions and data are offered in good faith but without guarantee as conditions and methods of use of our products are beyond our control. All claims must be made within 30 days following the date of delivery. The prospective user must determine the suitability of our materials before adopting them on a commercial scale. Suggested uses of our products are not recommendations to use our products in violation of any patent or as a license under any patent of Rockland Immunochemicals, Inc. If you require a commercial license to use this material and do not have one, then return this material, unopened to: Rockland Inc., P.O. BOX 5199, Limerick, Pennsylvania, USA.